ChemComm

COMMUNICATION

View Article Online
View Journal | View Issue

Cite this: *Chem. Commun.*, 2023, 59, 3846

Received 15th February 2023,
Accepted 1st March 2023

DOI: 10.1039/d3cc00710c

rsc.li/chemcomm

Cooperative dihydrogen activation at a Na(I)$_2$/Mg(I)$_2$ ensemble†

Han-Ying Liu, Samuel E. Neale, Michael S. Hill,* Mary F. Mahon, Claire L. McMullin* and Benjamin L. Morrison

[{SiN^{Dipp}}MgNa]$_2$ ({SiN^{Dipp}} = {CH$_2$SiMe$_2$N(Dipp)}$_2$; Dipp = 2,6-i-Pr$_2$C$_6$H$_3$) reacts directly with H$_2$ to provide a heterobimetallic hydride. Although the transformation is complicated by the simultaneous disproportionation of magnesium, computational density functional theory (DFT) studies suggest that this reactivity is initiated by orbitally-constrained $\sigma_{Mg-Mg} \rightarrow \sigma^*_{H-H}$ and $\sigma_{H-H} \rightarrow n^*_{Na(3s)}$ interactions between the frontier MOs of both H$_2$ and the tetrametallic core of [{SiN^{Dipp}}MgNa]$_2$.

The binding and cleavage of the strong (436 kJ mol^{-1}) H–H σ-bond of dihydrogen at mid and late transition metal centres provided a fulcrum for both a fundamental understanding of d-block complex reactivity and the development of numerous catalytic and stoichiometric processes.[1,2] This chemistry is enabled by the narrowly spread manifold of nd valence orbital energies involved in the synergic activation of the H$_2$ molecule (Fig. 1a).

As articulated in Power's influential review of 2010,[3] typical s- and p-block compounds do not generally display the modest separation in valence orbital energies ($\leq$4 eV) required to effect similar interactions. From 2005 onwards, however, it was shown that a selection of multiply bonded and carbenoid compounds derived from, primarily, the heavier elements of group 13–15 in low formal oxidation states can provide frontier orbitals with an energetic and spatial disposition appropriate for H–H oxidative addition (Fig. 1b and c).[4–7] Although semantics might identify frustrated Lewis pairs (FLPs) as a separate sub-category of main group chemistry,[8,9] a commonly considered mode of H$_2$ activation (Fig. 1d) attributes a significant degree of complementarity.[10] From this viewpoint, therefore, the reactivity of an FLP toward dihydrogen may be rationalised in an analogous manner, albeit one in which the frontier orbitals are introduced as spatially separated basic (HOMO) and acidic (LUMO) components.

There is now significant precedent for orbitally unconstrained (*i.e.* highly polarised) H–H σ-bond metathesis at the Ae–X (Ae = alkaline earth, Mg, Ca, Sr, Ba) bonds of group 2 derivatives in their conventional 2+ oxidation state.[11] The thermodynamic viability of H$_2$ addition to the Mg–Mg bonds of Jones and co-workers' β-diketiminato (*e.g.* **1–3**, Fig. 2) and guanidinato Mg(I) complexes ($\Delta H \approx$ 24 kcal mol^{-1}) was also assessed soon after their initial report in 2007.[12] Despite the synthesis of more than 20 further comparable species, however, and an intense exploration of Mg(I) compounds as potent reducing reagents,[13] reductive H$_2$ activation at an isolable Mg–Mg bonded molecule, either thermal or photoactivated, remains to be described.[14] In contrast, Harder and co-workers have recently reported that treatment of both the unique Mg(0) species, [(BDI*)MgNa]$_2$ (**4**; BDI* = HC{C(*t*-Bu)N(DiPeP)}$_2$; DiPeP = 2,6-(3-pentyl)-phenyl) and the mixed oxidation state [Mg(I)/Mg(0)] compound, [(BDI*)MgMgMg(BDI*)] (**5**), derived therefrom, with H$_2$ (1.5 bar) generates the magnesium hydride, [(BDI*)MgH] (**3**) in *ca.* 30% isolated yield (Fig. 2).[15] Although no further products were identified from the reaction of **4**, the

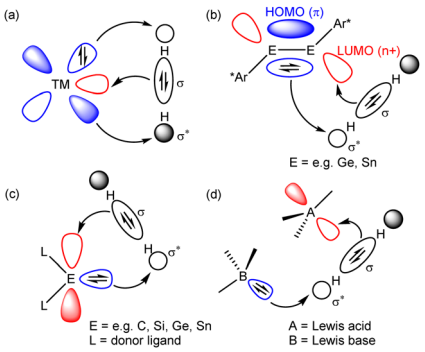

Fig. 1 Modes of synergic H$_2$ activation by (a) a typical late transition metal, (b) heavier group 14 element alkyne analogues, (c) tetrelenes and (d) an archetypal FLP.

Department of Chemistry, University of Bath, Claverton Down, Bath, BA2 7AY, UK. E-mail: msh27@bath.ac.uk, cm2025@bth.ac.uk

† Electronic supplementary information (ESI) available: General synthetic experimental details, NMR spectra, X-ray analysis of compound **9**, details of the computational analysis and atomic coordinates. CCDC 2217279. For ESI and crystallographic data in CIF or other electronic format see DOI: https://doi.org/10.1039/d3cc00710c

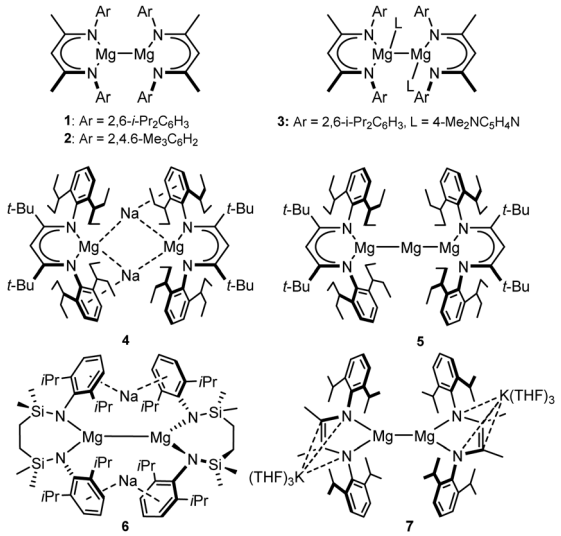

Fig. 2 Selected examples of Mg–Mg bonded magnesium(I) derivatives.

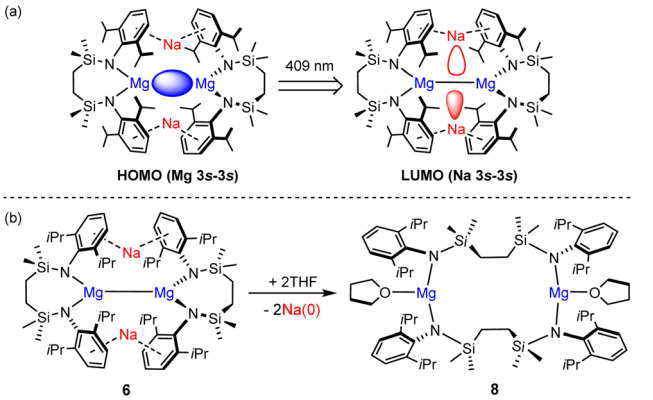

Fig. 3 (a) Representations of the calculated frontier molecular orbitals of **6**; (b) reactivity of compound **6** toward THF to form **8** and elemental sodium.

transformation of **5** was noted to result in the extrusion of metallic magnesium. In neither case, however, was the potential mode of H_2 activation assessed.

Inspired in part by the synthesis of **4**, we have described the topologically-related, [{SiN^{Dipp}}MgNa]$_2$ (**6**; [{SiN^{Dipp}} = {CH$_2$SiMe$_2$N(Dipp)}$_2$; Dipp = 2,6-i-Pr$_2$C$_6$H$_3$)] (Fig. 2).[16] Although **6** bears a resemblance to the previously reported species of Yang and co-workers (*e.g.* **7**),[17] the redox-innocence of the {SiN^{Dipp}} ligands and the *N*-aryl encapsulation of the sodium cations provides significant electronic discrimination. This is reflected in the structure of **6** through an elongation of the Mg–Mg bond [3.2124(11) Å (**6**) *versus* 2.9370(18) Å (**7**)]. Computational (NBO, QTAIM) analysis also identified a degree of electronic cooperativity between the magnesium and sodium centres. This manifests as a pronounced yellow colour arising from an absorption at 409 nm (3.0 eV) attributed to a transition between the Mg–Mg σ-bond (HOMO), arising from overlap of the magnesium 3s wavefunctions, and a LUMO largely represented by an out-of-phase combination of the sodium 3s atomic orbitals (Fig. 3a).[18]

The behaviour of **6** supports an interpretation of its bonding as a tetrametallic ensemble. Most strikingly, treatment with non-reducible bases such as THF (Fig. 3b) results in the selective extrusion of metallic sodium and oxidation of the Mg(I) centres to the more conventional Mg(II) state.[18] Although these processes are also characterised by a structural reorganisation of the chelated diamide spectator ligand to form the macrocyclic species **8**, computational studies indicated that intramolecular electron transfer is expedited *via* the Mg(I)-derived HOMO and Na(I)-derived LUMO. The narrow separation in energy between these frontier orbitals (*ca.* 3 eV) is more reminiscent of the low oxidation state p-block species (typically 2–3 eV) depicted in Fig. 1b and c than previously reported Mg–Mg bonded derivatives ($\geq$4 eV).[12] With these observations in mind, therefore, it was speculated that the alkali metal-centred frontier orbitals of **6** may also facilitate a cooperative reaction with H_2.

Although treatment of a degassed benzene solution of **6** with H_2 (2 bar) provided no evidence of an observable reaction over 12 hours at room (*ca.* 25 °C) temperature, monitoring by ^{1}H NMR spectroscopy indicated conversion to a predominant new compound (**9**) was induced after heating at 40 °C for 3 days. This process occurred with the formation of a black metallic precipitate. Compound **9** was isolated as colourless single crystals from hexane at room temperature. The resultant X-ray diffraction analysis (Fig. 4) revealed that compound **9** is a centrosymmetric heterobimetallic hydride species. The hydride ligands of **9** were located and refined with a riding U_{iso} value to be trigonally encapsulated by a still chelated diamidomagnesium centre and two sodium cations. The sodium atoms are bound in a η^6-fashion by each of the Dipp substituents of the chelated {SiN^{Dipp}} ligands, but are differentiated by their interactions with an additional diamide dianion that now adopts a {Na2-μ-κ^1-*N*,μ-κ^1-*N*′-Na2′} bridging mode reminiscent of those to Mg in the macrocyclic species **8**.[18] While Na1/Na1^1 engage *via* further polyhapto interactions with C31–C36 (and C31^1–C36^1) comprising the Dipp substituents of the bridging dianion, the coordination spheres of Na2/Na2^1 are completed by N3/N3^1. The Mg1–N1 [1.9795(13) Å] and Mg1–N2 [1.9711(14) Å] bonds of **9** are significantly shorter than the Mg–N distances observed in **6** (avg. 2.08 Å),[16] consistent with the oxidation of Mg(I) to Mg(II). While several amido-derived Na/Mg hydrides have been reported to result from either β-C–H elimination or metal amide/Si–H metathesis,[19] compound **9** is the first such species in which the hydride ligands arise from the direct activation of dihydrogen. Although its presence could not be identified by ^{1}H NMR spectroscopy in d_6-benzene solution, dihydrogen was confirmed as the source of the hydride ligands of **9** by performance of a further reaction of **6** with D_2. This latter process provided similar observations and resulted in the isolation of **9**-d_2, which was characterised by a singlet signal at δ 4.16 ppm as the sole observable resonance in its ^{2}H NMR spectrum in benzene.

Acid digestion and quantitative analysis by ICP-OES revealed that the solid residue deposited during the reaction of **6** with H_2 comprised magnesium as the sole constituent s-block metal

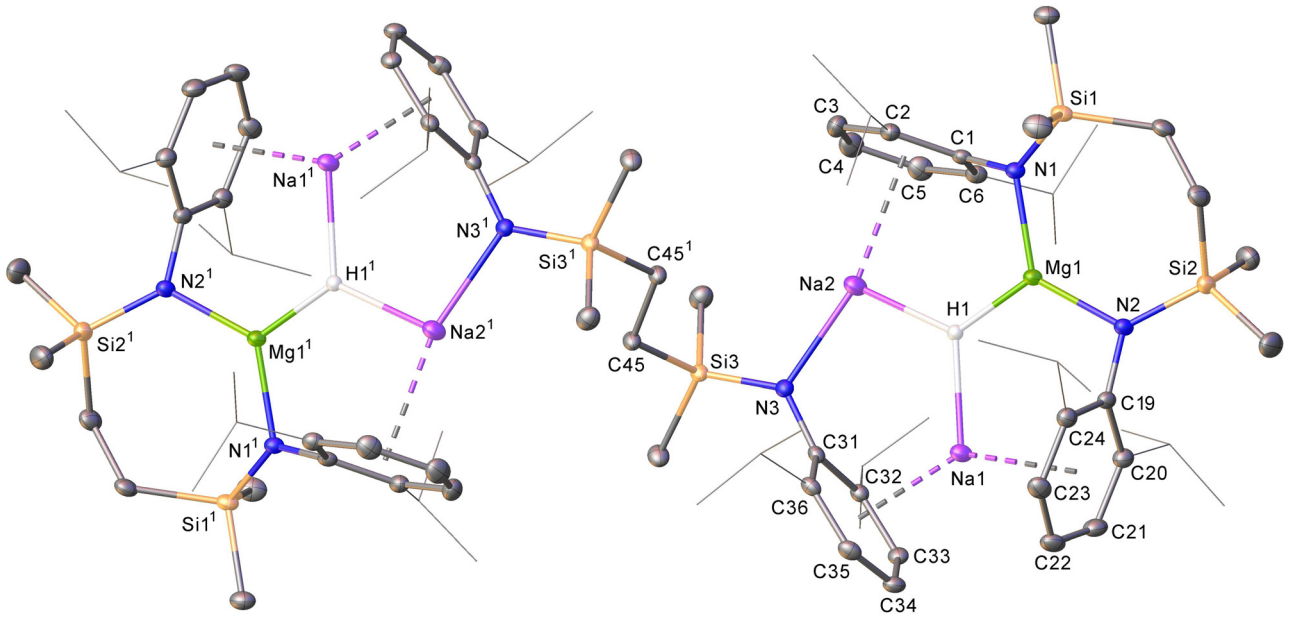

Fig. 4 Displacement ellipsoid (30% probability) plot of compound **9**. H atoms, apart from H1 and H1¹, and occluded hexane solvent have been omitted and iso-propyl groups are shown as wireframe for clarity. Selected bond lengths (Å) and angles (°): Mg1–N1 1.9795(13), Mg1–N2 1.9711(14), Na1–C22 2.7776(18), Na1–C33 2.7840(16), Na1–C34 2.7344(16), Na2–N3 2.2895(14), Na2–C1 3.1096(16), Na2–C2 3.0148(17), Na2–C3 2.9391(19), Na2–C4 2.948(2), Na2–C5 3.023(2), Na2–C6 3.1209(18), N1–Mg1–N2 126.44(6), N1–Mg1–N2 126.44(6). Operations to generate symmetry equivalent atoms: $1-x, 2-y, 1-z$.

with levels of sodium below the detection limit of the technique (see ESI†). Furthermore, the quantity of magnesium was consistent with the reaction stoichiometry shown in eqn (1), which we surmise results from the formal disproportionation of the Mg(I) centres of compound **6**.

While we cannot yet discount alternative polarised metathesis or radical-based pathways,[11,14] these deductions infer that the frontier orbital interactions invoked in the initial coordination of H_2 to **6** bear some analogy to those of the generalised d- and p-block-derived systems depicted in Fig. 1. The semi-

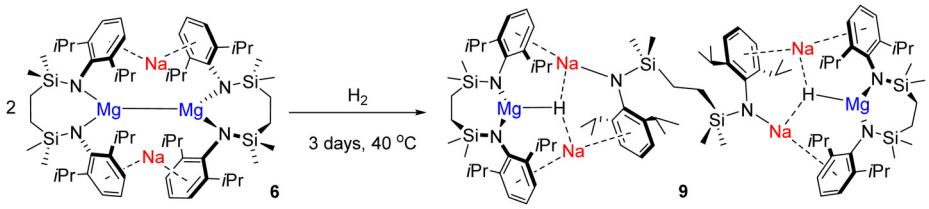

(1)

DFT calculations (BP86-D3BJ/BS2(benzene)//BP86/BS1 level of theory, see the ESI† for full details) were performed to assess the kinetics of H_2 addition to **6** (denoted as **I** in the computational study) and the structure of the resulting H_2 adduct. Initial H_2 addition was identified to take place *via* **TS(I–II)** and a barrier of +18.5 kcal mol^{-1} to form **II** (+14.1 kcal mol^{-1}). Subsequent H_2 reorientation *via* a low-lying saddle point, **TS(II–III)** (+13.6 kcal mol^{-1}), affords a more stable adduct, **III** (+11.0 kcal mol^{-1}), in which a terminus of the H_2 molecule is directed towards the Mg–Mg σ bond (Fig. 5a).[20]

NBO-based donor–acceptor interaction analysis of **III** reveals two appreciable interactions between H_2 and the tetrametallic Mg_2Na_2 unit; a $\sigma_{Mg-Mg} \rightarrow \sigma^*_{H-H}$ interaction ($\Delta E^{(2)}$ = 9.2 kcal mol^{-1}; Fig. 4b) supplemented by a subtle but still significant engagement *via* $\sigma_{H-H} \rightarrow n^*_{Na(3s)}$ ($\Delta E^{(2)}$ = 1.6 kcal mol^{-1}; Fig. 5c).

heterogeneous nature of the Mg(0) extrusion process and the structural complexity of **9**, however, dictate that the onward process does not lend itself to further prudent mechanistic analysis.

These combined experimental and theoretical results imply that the H_2 activation process invoked through its interaction with **6** may be rationalised as a consequence of the frontier orbitals arising from the low oxidation state assembly of the two dissimilar s-block elements (Fig. 3a). This perspective serves to further discriminate the chemistry of the low oxidation state heterobimetallic species, **6**, from that so far deduced for the previously described Mg–Mg bonded Mg(I) derivatives (*e.g.* **1–3** and **7**).[12,13] Similarly, the conceptual framework provided by the intermediate **III** signposts a potential ability to manipulate the frontier orbitals of related systems toward even more challenging small molecule transformations through the

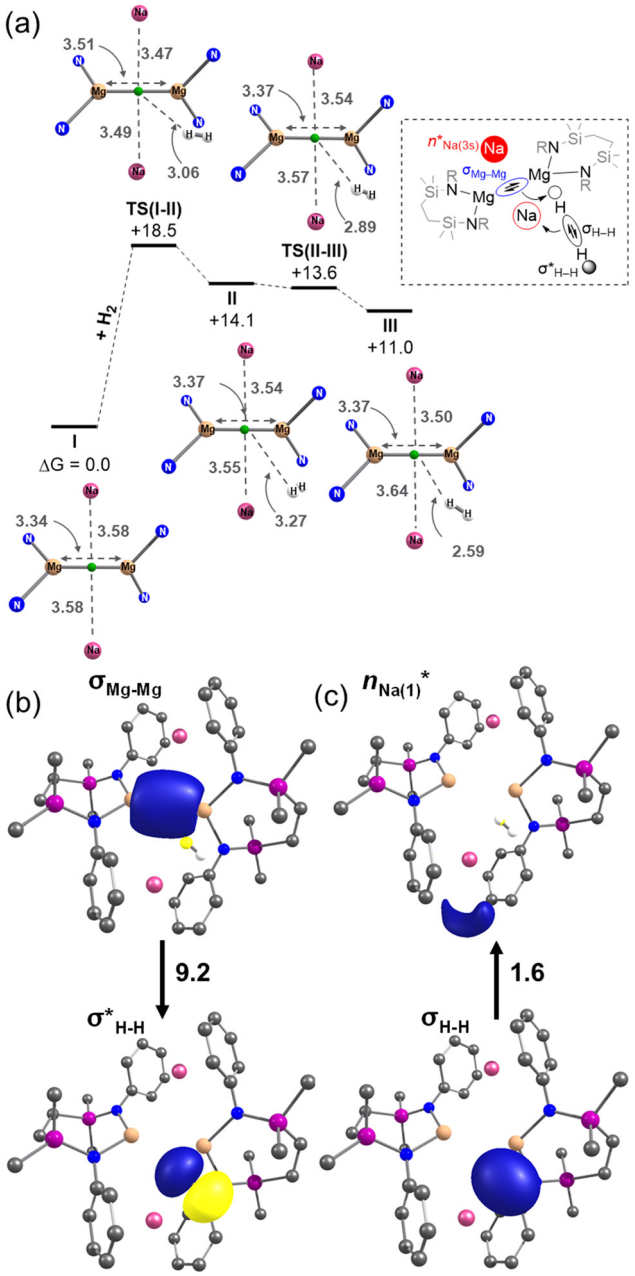

Fig. 5 (a) Computed free energy profile (BP86-D3BJ/BS2(benzene)//BP86/BS1), in kcal mol^{-1} for initial addition of H_2 to **6**/**I**. (SiN^{Dipp} ligand backbone and aromatic rings removed for clarity, and interatomic distances, and distances between each Na and the Mg–Mg midpoint (green) quoted in Å). (b) $\sigma_{Mg-Mg} \rightarrow \sigma^*_{H-H}$ interaction of **III**, identified by second-order perturbation energy analysis of the Fock matrix in NBO basis; (c) the corresponding $\sigma_{H-H} \rightarrow n^*_{Na(3s)}$ interaction of **III**. The donor–acceptor interaction energies, $\Delta E^{(2)}$, are quoted in kcal mol^{-1}.

templated assembly of further low oxidation state arrays of dissimilar s-block element centres. We are continuing to explore these possibilities with a broader scope of complex types, metal identities and small molecule substrates.

HYL performed the synthesis and characterisation of the new compounds reported. MSH and CLM conceptualised the study and finalised the manuscript for submission. SEN and BLM performed the computational analysis and MFM finalised the X-ray diffraction analysis of **9** for publication.

We thank the EPSRC (EP/R020752/1) for support of this research. This research made use of the Balena and Anatra High Performance Computing (HPC) Services at the University of Bath. (University of Bath, Research Computing Group, DOI: https://doi.org/10.15125/b6cd-s854).

Conflicts of interest

There are no conflicts to declare.

Notes and references

1 G. J. Kubas, *Acc. Chem. Res.*, 1988, **21**, 120–128.
2 G. J. Kubas, *J. Organomet. Chem.*, 2009, **694**, 2648–2653.
3 P. P. Power, *Nature*, 2010, **463**, 171–177.
4 T. Chu and G. I. Nikonov, *Chem. Rev.*, 2018, **118**, 3608–3680.
5 C. Weetman and S. Inoue, *ChemCatChem*, 2018, **10**, 4213–4228.
6 G. H. Spikes, J. C. Fettinger and P. P. Power, *J. Am. Chem. Soc.*, 2005, **127**, 12232–12233.
7 Y. Peng, M. Brynda, B. D. Ellis, J. C. Fettinger, E. Rivard and P. P. Power, *Chem. Commun.*, 2008, 6042–6044.
8 G. C. Welch, R. R. S. Juan, J. D. Masuda and D. W. Stephan, *Science*, 2006, **314**, 1124–1126.
9 F. G. Fontaine and D. W. Stephan, *Philos. Trans. R. Soc., A*, 2017, **375**, 20170004.
10 T. A. Rokob, I. Bako, A. Stirling, A. Hamza and I. Papai, *J. Am. Chem. Soc.*, 2013, **135**, 4425–4437.
11 H. Bauer and S. Harder, in *Early Main Group Metal Catalyzed Hydrogenation, in Early Main Group Metal Catalysis: Concepts and Reactions*, ed., S. Harder, 2020, pp. 175–199.
12 (*a*) S. P. Green, C. Jones and A. Stasch, *Science*, 2007, **318**, 1754–1757; (*b*) A. Datta, *J. Phys. Chem. C*, 2008, **112**, 18727–18729.
13 For a recent review, seeL. A. Freeman, J. E. Walley and R. J. Gilliard, *Nat. Synth.*, 2022, **1**, 439–448.
14 Here, we draw a demarcation between such divalent {Mg–Mg}-bonded Mg(I) compounds and radicular Mg(I) species. Notably, a recent report by Harder and co-workers has highlighted that ball milling of K/KI and [(BDI)MgI(OEt$_2$)] under H_2 provides a ca. 1.3 : 1.0 mixture of compound **1** and [(BDI)MgH]$_2$. While compound **1** remains unreactive, the latter species is interpreted to result from the generation and persistence of highly reactive 'unquenched' [(BDI)Mg$^\bullet$], radicals under the solvent-free conditions and which are then reactive toward H_2. See: (*a*) D. Jędrzkiewicz, J. Langer and S. Harder, *Z. Anorg. Allg. Chem.*, 2022, **648**, e202200138. The hydrogenation of Mg(I) dimers using 1,3-cyclohexadiene has also been described. See: (*b*) R. Lalrempuia, C. E. Kefalidis, S. J. Bonyhady, B. Schwarze, L. Maron, A. Stasch and C. Jones, *J. Am. Chem. Soc.*, 2015, **137**, 8944–8947.
15 B. Rösch, T. X. Gentner, J. Eyselein, J. Langer, H. Elsen and S. Harder, *Nature*, 2021, **592**, 717–719.
16 H. Y. Liu, R. J. Schwamm, S. E. Neale, M. S. Hill, C. L. McMullin and M. F. Mahon, *J. Am. Chem. Soc.*, 2021, **143**, 17851–17856.
17 Y. Liu, S. Li, X.-J. Yang, P. Yang and B. Wu, *J. Am. Chem. Soc.*, 2009, **131**, 4210–4211.
18 H.-Y. Liu, S. E. Neale, M. S. Hill, M. F. Mahon, C. L. McMullin and E. Richards, *Angew. Chem., Int. Ed.*, 2023, **62**, e202213670.
19 (*a*) D. J. Gallagher, K. W. Henderson, A. R. Kennedy, C. T. O'Hara, R. E. Mulvey and R. B. Rowlings, *Chem. Commun.*, 2002, 376–377; (*b*) D. V. Graham, A. R. Kennedy, R. E. Mulvey and C. T. O'Hara, *Acta Crystallogr., Sect. C: Cryst. Struct. Commun.*, 2006, **62**, M366–M368; (*c*) D. J. Liptrot, M. S. Hill and M. F. Mahon, *Chem. – Eur. J.*, 2014, **20**, 9871–9874; for a review, see: (*d*) M. M. D. Roy, A. A. Omaña, A. S. S. Wilson, M. S. Hill, S. Aldridge and E. Rivard, *Chem. Rev.*, 2021, **121**, 12784–12965.
20 Based on the electronic energy, **TS(II–III)** is 0.1 kcal higher than **II** with one imaginary frequency of −58.5 cm^{-1}. Corrections have stabilised this TS structure relative to the zero species more than intermediate **II**.